Unexpected mechanochemical complexity: distinct reaction mechanisms in disulfide bond reduction in alkaline solution

Przemyslaw Dopieralski(1,2),* Jordi Ribas–Arino(1,3),†
Padmesh Anjukandi(1), Martin Krupicka(1,4), and Dominik Marx(1)
(1) *Lehrstuhl für Theoretische Chemie, Ruhr–Universität Bochum, 44780 Bochum, Germany*
(2) *Permanent Address: Faculty of Chemistry, University of Wroclaw, Joliot–Curie 14, 50-383 Wroclaw, Poland*
(3) *Current Address: Departament de Química Física and IQTCUB,*
Universitat de Barcelona, Av. Diagonal 645, 08028, Barcelona, Spain
(4) *Current Address: Max-Planck-Institut für Chemische Energiekoversion,*
Stiftstr. 34–36, 45470 Mülheim an der Ruhr, Germany

The reduction of disulfides has broad importance in chemistry, biochemistry and materials science, in particular upon mechanochemical activation. Here, isotensional simulations disclose that strikingly different mechanisms govern disulfide cleavage depending on external force. Crucial are desolvation and resolvation processes, which directly impact on activation free energies. The preferred pathway up to moderate forces, a bimolecular $\mathrm{S_N2}$ attack of $\mathrm{OH^-}$ at sulfur, competes with unimolecular C–S bond rupture at about 2 nN, while the latter even becomes barrierless beyond. Moreover, our study brings to light a surprisingly rich reactivity scenario that includes the transformation of $\mathrm{S_N2}$ pathways into pure bond breaking pathways at forces within the range of 1.2 to 2.2 nN. Given that these forces are easily reached in experiments, these insights will fundamentally change our understanding of mechanochemical activation in general, which is now expected to be considerably more intricate than previously thought.

Disulfide bond reduction is one of the most studied classes of reactions in the context of covalent mechanochemistry.[1–5] Following the pioneering force-clamp AFM study of the thiolate/disulfide exchange reaction[6], the effect of tensile forces on the kinetics and reaction mechanisms of disulfide bond reductions has been intensively investigated by means of single-molecule force spectroscopy,[7–15] molecular force probes[16,17] and computational studies.[18–26] All the efforts undertaken to decipher the intricacies of the coupling of mechanical stress and disulfide reactivity are not only very important from a fundamental science point of view, but also for biochemistry and polymer–based materials science and technology. In the context of biochemistry, there is growing evidence that the reduction of so-called "disulfide switches", usually found in protein regions of pronounced mechanical strain,[27] can trigger specific functions in proteins.[28–31] In a vastly different field, namely polymer science and technology, it has been demonstrated that devulcanization of rubber waste, being a pressing economic and environmental challenge faced by industry worldwide,[32] can be sustainably achieved by means of mechanochemical procedures in which the cleavage of covalent di– or polysulfide crosslinks is induced by mechanical stress.[32–34] Moreover, the force–induced breaking of sulfur-based cross-linkers plays a prime role in the mechanical fatigue of rubber and thus determines their life cycle.[35,36] Closely related to this, recent work strongly suggests that the use of disulfide bridges as dynamic linkages (being bonds that can form new crosslinks after cleavage) and "sacrificial bonds" (which selectively break more easily than others thus dissipating mechanical energy before fracture sets in) will most likely be at the forefront in the development of self–healable molecular materials capable of withstanding extreme mechanical stress.[37,38]

It is thus clear that our molecular understanding of the mechanochemistry of disulfide bridges is not only crucial in the realm of disulfide biochemistry, for instance to decipher the mechanisms employed by nature to control the activity of specific proteins, but can have a significant impact on technological applications of polymers as molecular materials including their sustainable recycling.

In a milestone experiment, a force–clamp AFM investigation of the mechanically activated cleavage of a protein disulfide bond through reaction with hydroxide ions, $\mathrm{OH^-(aq)}$, has been performed in aqueous solution.[10] These experiments uncovered a puzzling abrupt change in the reactivity at a force of about 0.5 nN, above which the accelerating effect of tensile force on the reaction rate is substantially reduced. Based on *ab initio* molecular dynamics (AIMD) simulations,[39] we only recently traced this "mechanochemical switch" back to the subtle interplay between two antagonistic effects caused by the external force;[24] see Supporting Information for summary. Subsequently, the underlying concept of force-induced steric hindrance has been shown to be of broader importance beyond just disulfides.[40]. The $\mathrm{S_N2}$ mechanism observed by our simulations in the low–force regime,[24] which is characterized by a direct attack of the solvated $\mathrm{OH^-}$ ion to one of the sulfur atoms, is in line with the mechanism proposed to interpret the force–clamp AFM results.[10] Moreover, it agrees with the mechanism of alkaline thermal decomposition of cystine or other aliphatic disulfides[41] and applies to thiolate/disulfide exchange in solution as well.[42–45]

Although computer simulations have provided a rationale for the enigmatic "mechanochemical switch" discovered in experiment, there is still a crucial question open, namely if the same reaction mechanism operates in the high–force regime? In fact, there is old experimental evidence that even the traditional thermal reduction of disulfides in alkaline solution is a very complex process that is not governed by a single mechanism.[41] Moreover, a host of examples are now known from covalent mechanochemistry where application of tensile forces in the nano-Newton range do dramatically change reaction mechanisms.[5] This strongly suggests that alternative reaction channels might successfully compete at higher forces with the $\mathrm{S_N}2$ pathway.

Two alternative mechanisms that are immediately conceivable have been proposed to be operative in the thermal cleavage of some disulfides in basic media. Elimination processes, which are initiated by abstraction of a proton from the disulfide, seem to be the mechanism underlying alkaline degradation of dithiocarboxylic acids, certain cystine derivatives, specific alkyl disulfides and of disulfides embedded in some proteins.[41,46–48] Gas phase and computer experiments on the reaction of dimethyl disulfide with hydroxide ions have also shown that an elimination mechanism is the preferred reaction channel for this particular disulfide bond reduction.[49,50] The second conceivable mechanism, which has been put forward to explain the reactivity of disulfides with electron-withdrawing groups and multivalent atoms bonded to the α–carbon atoms of the disulfide[41,51], would be a nucleophilic attack of the $\mathrm{OH^-}$ ion to one of the α–carbon atoms neighboring the disulfide bridge. These alternative mechanisms underpin the complexity already of the thermal alkaline disulfide bond reduction and highlight the lack of a detailed understanding of its mechanistic intricacies. At this point, it should be mentioned that the thiolate/disulfide exchange reaction has also its own intriguing subtleties. A proof of this is that several reactions of this type imply an addition–elimination pathway, rather than an S_N2 mechanism, when occurring in the gas phase.[43,52] In more general terms, it should also be stressed that recent investigations of nucleophilic attacks on S–S bridges continue to reveal unexpected reaction mechanisms.[53]

It is evident that putative reaction scenarios become even more intricate when mechanochemical activation comes into play. Indeed, external forces can activate new reactions channels, among which C–S or S–S bond rupture without the direct intervention of $\mathrm{OH^-}$ are apparently the most plausible options. Such rupture events were previously generated in computational studies[22,23], which merits some discussion. Therein, exceedingly large force–loading rates were employed in order to drive the disulfide bond cleavage in the picosecond or nanosecond time scales, which are unphysically short compared to force-clamp AFM. It is known that this particular approach most likely gives rise to non–equilibrium phenomena[5] and it is not clear whether the observed events are artifacts of "overstressing" the disulfides or whether they reflect their true chemistry. In fact, the force–field simulations[22] showed that the mechanism very much depends on the time scale as imposed by the biasing potential. But regardless of whether the reported bond ruptures are simulation artifacts or not, there is a core issue that still remains completely unresolved, namely, if the forces where these reaction channels might become competitive with the $\mathrm{S_N}2$ pathway are relevant to experiment or not.

Results

On the basis of a computational study that combines AIMD simulations[39] in the liquid phase together with enhanced sampling techniques, we elucidate in the following which reaction mechanisms become operative depending on the force regime. The model system chosen to investigate all reaction pathways of Figure 1 consists of one diethyl disulfide molecule placed in a cubic supercell together with one hydroxide anion and 70 water molecules to properly solvate the reactants subject to periodic boundary conditions. All simulations were performed using isotensional conditions,[54] which means that they were carried out in the presence of different but *constant* external tensile forces.[5] These tensile forces act on the two β–carbon atoms at the termini of the diethyl disulfide molecule and are applied along a fixed direction in space. For every value of the external force, the use of metadynamics or thermodynamic integration sampling yields a distinct force–transformed free energy surface (FES).[55]

Using this approach (see Supporting Sections I, II and III for details), the following five distinctly different reaction mechanisms (see Figure 1) have been studied in detail: (i) $\mathrm{S_N}2$ nucleophilic attack of $\mathrm{OH^-}$ to a sulfur atom (dubbed $\mathrm{S_N}2$ at sulfur), (ii) simple C–S bond cleavage, (iii) pure S–S rupture, (iv) $\mathrm{S_N}2$ nucleophilic attack of $\mathrm{OH^-}$ to a α–carbon atom ($\mathrm{S_N}2$ at α–carbon), and (v) α–elimination across the sulfur–sulfur bond with the abstraction of one proton from a α–carbon atom.

Nucleophilic attack of $\mathrm{OH^-}$ at sulfur

This "$\mathrm{S_N}2$ at S" reaction mechanism has been the focus of a previous study[24] on the mechanochemical disulfide switch.[10] We refer to Section V.A in the Supporting Information for pertinent details, but recall the salient features here to set the stage. This mechanism is the preferred one in the thermal limit and applying an external tensile force results in a notable overall decrease of the activation free energy from $\Delta A^\ddagger(F = 0) \sim 27$ kcal/mol down to ~ 11 kcal/mol at $F = 2$ nN as shown in Figure 1. The abrupt deceleration at around 0.3–0.4 nN, which explains the behavior discovered in experiment,[10] originates in a mechanically–induced conformational change[40] of the S–S–C–C dihedral angle of the disulfide moiety (and not C–S–S–C) from "open" to "closed".[24] Here, in contrast, the focus is on the high-force regime. The first remarkable finding of our exploration of the reactivity in this regime is that the bimolecular "$\mathrm{S_N}2$ at S" channel transforms into a unimolecular S–S bond cleavage for forces larger than *ca.* 2.25 nN (see Figure SI 5). This is the reason for which the red curve in Figure 1 is displayed only until it reaches the S–S bond scission channel at about 2.25 nN. Besides the unveiled transformation of the $\mathrm{S_N}2$ mechanism into the S–S bond cleavage mecha-

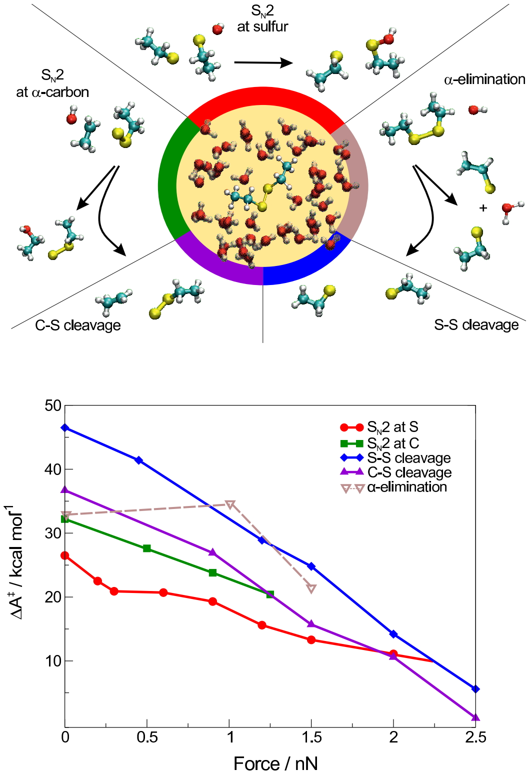

FIG. 1: **Force–dependence of the computed activation free energy, $\Delta A^{\ddagger}(F)$, for all five depicted reaction pathways.** *Top panel*: Scheme of the five different reaction pathways considered in this study. The central picture displays the model system employed in the simulations, which includes a diethyl disulfide molecule, an OH$^-$ ion and 70 water molecules all treated explicitly at the full electronic structure level. Note that for the pure C–S and S–S bond breaking mechanisms, the nucleophilic OH$^-$ ion is not involved in the reaction but it is present in the simulation box for consistency. *Bottom panel*: Force dependence of the activation free energies at 300 K for all the reaction channels described in the top panel; the "$\mathrm{S_N}2$ at S" data up to 2.0 nN have been taken from Figure 1a in Ref. 24. The color code used in these curves corresponds to the color code introduced in the top panel. Note that the computed data (displayed using different symbols) are connected with lines to guide the eye. The red line shown after the right–most red circle is an extrapolation (see main text for further details).

nism, our simulations also reveal that the former channel will be be overridden by yet another pathway beyond 2 nN, *vide infra*.

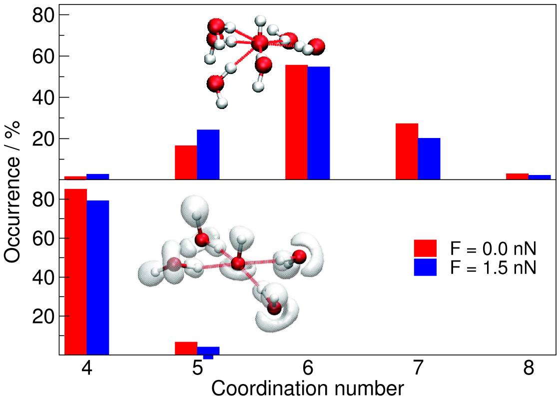

FIG. 2: **Solvation of the OH$^-$ nucleophile by water studied as a function of external force using the rigorous all–QM AIMD approach and a QM/MM hybrid MD approximation.** Comparison between the first hydration shell of OH$^-$(aq) close to the reactant state of its nucleophilic attack at sulfur (both at $F = 0$ and 1.5 nN) as obtained from AIMD simulations (treating the full system with the BLYP density functional), see bottom panel, and hybrid simulations (using the SPC force field for all water molecules), see top panel. The insets depict snapshots of the characteristic hydration patterns observed during the simulations, which is four– and six–coordinated OH$^-$(aq) according to all–QM and QM/MM simulations in the bottom and top panels, respectively.

Nucleophilic attack of OH$^-$(aq) at sulfur, moreover, serves as a paradigm to bring to light the crucial importance of solvation effects upon comparing our rigorous all–QM results (as presented throughout this manuscript) to approximate QM/MM data where all water molecules have been modeled by a standard molecular mechanics (MM) force field (as explained in Section V.B in the Supporting Information). Firstly, in contrast with the all–QM results presented herein, the QM/MM free energy profiles are found to not feature any minima or plateaus associated with the reactant states in the wide range of values of the reaction coordinate that was considered (see Figure SI6). The absence of such minima has important consequences because it precludes a proper evaluation of the activation free energies as a function of force, $\Delta A^{\ddagger}(F)$, when using the computational much less demanding QM/MM approximation. Secondly, the transition state structures in the QM/MM simulations are completely different (in terms of their S–S bond distance and the distance between the oxygen of the hydrated OH$^-$ anion and the sulfur atom being attacked) from those obtained in the all–QM simulations (see Figure SI7).

The molecular underpinnings of this dramatic failure are unveiled with the help of Figure 2. The comparison demonstrates that the solvation shell of OH$^-$(aq) close to the reactant state of this chemical reaction qualitatively differs from the expected planar four–fold coordination[56] (reproduced by the AIMD simulation in the bottom panel, see also inset) when the QM/MM approximation is used, i.e. six–fold (see top inset). It is thus concluded that a proper treatment of the solvation of the reactant species along the entire reaction pathway is a most crucial ingredient in any reliable computational treatment of the reactions of interest here, and that any approach that does not account for that is bound to fail.

Moreover, the use of microsolvated cluster models supplemented with implicit solvation schemes to model the $\mathrm{S_N}2$ reaction entails even more severe problems.

In fact, the calculation of the activation energy of this reaction using a model comprising one diethyl disulfide molecule, an OH^- anion and four water molecules that microsolvate the reactants gives rise to an energy barrier that does not even correspond to the substitution reaction! The computed value rather corresponds to the deprotonation reaction of the water molecule that acts as a nucleophile together with the proton transfers through the artificial wire-like topology of four water molecules. It is noted that this conclusion is supported by earlier results[20], where a thiol–disulfide exchange reaction was studied using such microsolvation calculations. In broader terms, it is known that the use of microsolvation models with a manageable number of water molecules[8,20,43] seem to fail to reproduce the experimentally observed trends for nucleophilic substitution in general,[57] and specifically at sulfur.[58]

Simple S–S and C–S bond rupture processes

Keeping the importance of proper solvation in mind, we can now turn to the mechanisms that will compete with the S_N2 at S pathway in the limit of large forces. The activation free energies as a function of the mechanical force, $\Delta A^\ddagger(F)$, for the reaction channels involving pure S–S and C–S bond scissions were evaluated by using the S–S and the C–S bond distances as reaction coordinates, respectively. At this point, it should be mentioned that all these simple S–S and C–S bond scission processes observed in our simulations correspond to heterolytic bond cleavages (see Supporting Section IV C for analyses). The computed activation free energies at zero force are 47 kcal/mol and 36 kcal/mol, respectively (see Figure 1). Importantly, since both activation free energies are much higher than that of the S_N2 reaction involving one of the sulfur atoms (see Figure 1), it is safely concluded that the pure S–S and C–S bond scissions are not operative in the thermal limit.

The effect of tensile force on S–S and C–S bond rupture, however, is much more pronounced than on nucleophilic attack at sulfur, most notably at high forces. As clearly displayed in Figure 1, the activation free energies of these pathways at $F = 2.0$ nN are found to have dropped dramatically to about one third of the corresponding values at zero force. The marked force sensitivity of $\Delta A^\ddagger(F)$ for straightforward bond rupture implies that the coupling between the reaction coordinate and the mechanical coordinate is much more efficient in the S–S and C–S bond cleavage processes than in the S_N2 reaction.

In its turn, such efficient mechanochemical coupling in the case of pure bond scissions impacts decisively on the reactivity scenario in the limit of large forces. Indeed, the respective $\Delta A^\ddagger(F)$ curves compiled in Figure 1 bring to light that at $F \sim 2.0$ nN, the activation free energy of the C–S bond scission process not only competes but is even slightly lower than that of the S_N2 pathway and finally, at $F \sim 2.5$ nN, simple C–S rupture even becomes a virtually barrierless process. In other words, the mechanochemical events probed by force–clamp AFM experiments on a stretched disulfide bridge in basic media at high forces around 2 nN can be the result of both simple C–S bond rupture and a S_N2 nucleophilic attack reaction of an hydroxide anion to one of the sulfur atoms.

There is yet another prominent covalent bond that could simply be ripped apart by applying mechanical forces, namely the disulfide bond itself. In the purely thermal limit and also at low forces this pathway is by far highest in free energy of all five scenarios investigated according to the data collected in Figure 1. Even at $F = 2.0$ nN, the activation free energy for this S–S bond scission channel ($\Delta A^\ddagger = 14.2$ kcal/mol) is still considerably higher than that corresponding to either C–S bond rupture or to the S_N2 at S mechanism. Finally, at forces as large as $F = 2.5$ nN, the S–S bond scission channel continues to feature an appreciable barrier, $\Delta A^\ddagger \sim 6$ kcal/mol, in contrast with the C–S bond scission channel, whose $\Delta A^\ddagger$ value at that force is vanishingly small. The S–S bond cleavage pathway is thus not expected to be operative up to this specific force, although the associated activation free energy decreases steeply upon increasing the tensile force.

Nucleophilic substitution at an α-carbon

Yet another pathway involves nucleophilic attack of the OH^- anion at one of the α-carbons of the disulfide bridge. In order to compute the dependence of the activation free energies on force, $\Delta A^\ddagger(F)$, two collective variables were used in this case: d_{C-S} (the distance associated with the C–S bond that is cleaved upon addition of the OH^- nucleophile) and $d_{C\cdots OH^-}$ (the distance between the oxygen atom of the OH^- ion and the α-carbon being attacked, which was selected and fixed prior to the simulations).

In the thermal limit, the nucleophilic substitution at an α-carbon site of the disulfide is found to proceed also *via* an S_N2 mechanism (see free energy surface at $F = 0$ nN in Figure 3, where it is clearly shown that the reaction involves a simultaneous increase of d_{C-S} while $d_{C\cdots OH^-}$ decreases. However, the activation free energy of this "S_N2 at C" process is ∼6 kcal/mol higher than that of the nucleophilic substitution at sulfur as most clearly seen from the direct comparison in Figure 1. Hence, this mechanism – even if it is distinctly lower in free energy than the two simple C–S or S–S bond rupture processes – does not play any role under pure thermal activation, i.e. in the absence of additional mechanochemical activation.

Upon applying mechanical forces, this particular pathway follows an S_N2 mechanism akin to the thermal limit at $F = 0$ nN (see free energy surfaces at $F = 0.5$ nN and $F = 1.25$ nN of Figure 3) up to $F = 1.25$ nN. Although applying tensile force results in a considerable reduction of the activation free energy of this reaction channel, its $\Delta A^\ddagger(F)$ curve is found to always lie considerably above than that of the pathway involving the nucleophilic attack at sulfur (see Figure 1). It is therefore concluded that disulfide bond reduction as probed in the force–clamp AFM experiments cannot proceed by a nucleophilic attack on the α-carbon in the range of small to moderate forces.

In stark contrast, a most interesting phenomenon is detected upon reaching forces that exceed the critical value, $F \sim 1.25$ nN. For such forces, $F > 1.25$ nN, the addition of the OH^- nucleophile to the α-carbon does no longer occur in a single concerted step, but in two steps. The first step now is a pure C–S bond rupture process, while only the second one consists in the addition of the hydroxide ion, but to the carbocation that has been generated in the first step! This is most clearly visualized *via* the set of force–transformed FESs at selected forces as displayed in Figure 3. Obviously, only $d_{\mathrm{C-S}}$ changes in the first step of the reaction sequence, while the second step only implies a change of $d_{\mathrm{C\cdots OH^-}}$. These simulations thus reveal another example of a force–induced transformation of a concerted bimolecular mechanism into a two-step mechanism, in which the first step is a unimolecular bond breaking event.

At this point, it should be stressed that the final products of the process are always the same – irrespective of whether the reaction occurs concertedly or in two steps. Since the addition of OH^- to the carbocation is virtually a barrierless process, the activation free energy of the global process arises from the simple C–S bond rupture event! This is why it can be stated that the nucleophilic attack on an α–carbon collapses into a pure C–S bond rupture pathway for $F > 1.25$ nN. This is also the reason for which the activation free energy curves, $\Delta A^{\ddagger}(F)$, of both pathways perfectly merge at $F = 1.25$ nN and only the curve associated with the C–S bond rupture survives above that critical force (see Figure 1). Overall, the results reported in this subsection furnish yet another remarkable example of the dramatic changes that external forces can cause in the free energy landscapes corresponding to mechanochemically activated covalent reactions.

Elimination at an α–carbon

The α-elimination reaction mechanism was studied using two collective variables: $d_{\mathrm{C-H}} - d_{\mathrm{H\cdots OH}}$ and $d_{\mathrm{S-S}}$, where $d_{\mathrm{C-H}}$ is the distance between the disulfide proton that is abstracted and the carbon atom to which this proton is bonded in the reactant state, while $d_{\mathrm{H\cdots OH}}$ is the distance between the proton being abstracted and the attacking OH^- ion, whereas $d_{\mathrm{S-S}}$ is the distance between the two sulfur atoms.

Our simulations reveal that the α-elimination reaction follows in the thermal limit (see the free energy surface at $F = 0$ nN in Figure 4) a two–step mechanism: the first step is the proton abstraction process followed by the S–S bond rupture in terms of a second step. The first step is an activated process with an activation free energy of 33 kcal/mol (see Figure 1 and Figure 4), while the S–S bond rupture of the carbanion generated in the first step is an essentially barrierless process. It is thus concluded that the carbanion formed upon deprotonation is an unstable species that stabilizes itself by breaking the disulfide bond. Indeed, constrained AIMD simulations of exclusively the first step of the α-elimination reaction (using $d_{\mathrm{C-H}} - d_{\mathrm{H\cdots OH}}$ as the one-dimensional constrained reaction coordinate) resulted in an activation free energy of 29 kcal/mol (see Figure SI11) and therefore support this conclusion.

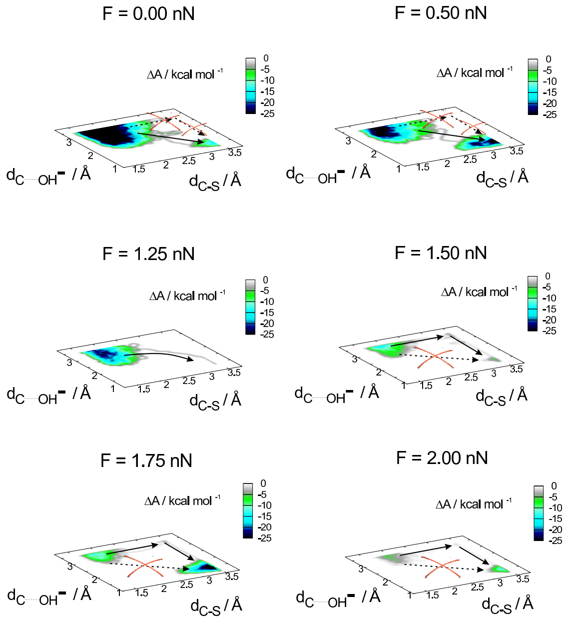

FIG. 3: **Change of the reaction mechanism from a concerted one–step reaction to a two–step process for the OH^- attack at an α–carbon.** Force–transformed free energy surfaces for the nucleophilic attack of OH^- to one of the α-carbon atoms of the disulfide bridge at several values of the external force at 300 K in aqueous solution. Black solid arrows highlight schematically the energetically preferred minimum free energy pathways according to the topology of the underlying free energy landscapes that depends on the magnitude of the constant external force, whereas dashed arrows and red crosses correspond to the disfavored mechanisms depending on force. Although the process is a standard S_N2 nucleophilic attack reaction in the thermal limit ($F = 0$ nN) and at low forces, straightforward C–S bond rupture sets in beyond the critical force, $F \sim 1.25$ nN, as demonstrated for $F = 1.50$, 1.75 and 2.00 nN.

As a result, the α-elimination reaction mechanism comes quite close to the lowest-energy pathway at $F = 0$ nN, which is the S_N2 nucleophilic attack of the OH^- ion to one of the sulfur atoms (for which $\Delta A^{\ddagger}(F = 0) \sim 27$ kcal/mol). This result suggests that the α-elimination pathway might even become the preferred mechanism at zero force if the α-hydrogen became more acidic due to the presence of electron-withdrawing groups placed nearby.

In striking contrast to the behavior featured by the force dependence of the activation free energy for all other reaction channels, the external tensile force leads to an increase in $\Delta A^{\ddagger}(F)$ in case of the α-elimination channel – and thus to its deceleration – at moderate forces. Specifically, at $F = 1.0$ nN, the activation free energy of this mechanism is 35 kcal/mol, which is not only higher than its barrier in the purely thermal activation limit, but also higher than these energies for all the alternative reaction pathways at that force. The AIMD trajectories provide insight into the origin of such an unusual increase of $\Delta A^{\ddagger}$ due to mechanical forces. As shown in Figure 4, an external force of $F = 1.0$ nN transforms the FES of the α-elimination channel in such a way that this reaction takes place via a concerted mechanism, in which the S–S bond scission occurs synchronously with the α–proton abstraction. Hence, the high barrier of this process originates in the simultaneous rupture of two different bonds as the reaction proceeds.

Astonishingly, the mechanistic scenario found at $F = 1.5$ nN is again markedly different, not only from that $F = 1.0$ nN but also from the thermal mechanism at zero force. At $F = 1.5$ nN, the α-elimination mechanism takes place in two successive steps, the first one being S–S bond scission while the second step being the deprotonation (see Figure 4). Hence, the order of the steps at $F = 1.5$ nN is seen to be reversed with respect to their sequence observed upon thermal activation.

Closely related to the α-elimination pathway, the cleavage of the disulfide bridge could also occur *via* a β-elimination process in which the OH^- ion removes a β-proton of the disulfide bridge. In this work, we have not considered the β-elimination channel due to the limited size of the model system, i.e. diethyl disulfide. However, in an independent publication[59] exclusively devoted to this pathway (in which we have used a larger model system), we have shown that its associated activation free energy lies much higher in energy than the "S_N2 at S" pathway in the whole range of forces. Therefore, the β-elimination channel can not compete with the "S_N2 at S" channel at any force.

Discussion

The key finding of this study, unveiled by large-scale computer simulations, is the unexpected complexity of disulfide bond reduction that is generated upon mechanochemical activation as induced by tensile forces. This complexity is embodied in the force–dependence of free energy landscapes of vastly different reaction pathways obtained by means of advanced *ab initio* molecular dynamics at constant external force in the liquid phase. In particular, the following five distinct reaction scenarios have been studied in detail: two S_N2 mechanisms involving nucleophilic attack of an OH^- ion at either sulfur or α-carbon atoms of the disulfide bond, direct rupture of both the S–S and C–S bonds, as well as an α–elimination process across the sulfur–sulfur bond.

Although cleavage of the disulfide bridge is known to proceed exclusively *via* nucleophilic attack of OH^- to one of the sulfur atoms in the thermal limit, the different coupling between finite tensile forces and the particular reaction coordinate of each mechanism leads to pronounced differences in how the pathways and thus the activation free energies respond to external stress. This leads to a markedly rich force-dependent reactivity scenario in the nano-Newton force regime. The largest couplings between force and reaction coordinate are observed for the simple S–S and C–S bond scissions, where these bonds are ripped apart in a brute force manner. Because of this, the rate at which the activation free energies of these two pathways decrease with the force, and thus their force–responses, is larger than in any other reaction scenario. As a result, the activation free energies of these reaction channels get rapidly closer to that of S_N2 attack on sulfur as the force increases. Still, the energetic gap of this lowest-lying S_N2 mechanism and all other mechanisms is considerable up to forces of roughly one nN. Hence, the disulfide bond cleavage continues to be governed by the nucleophilic substitution at sulfur by OH^- in the low–

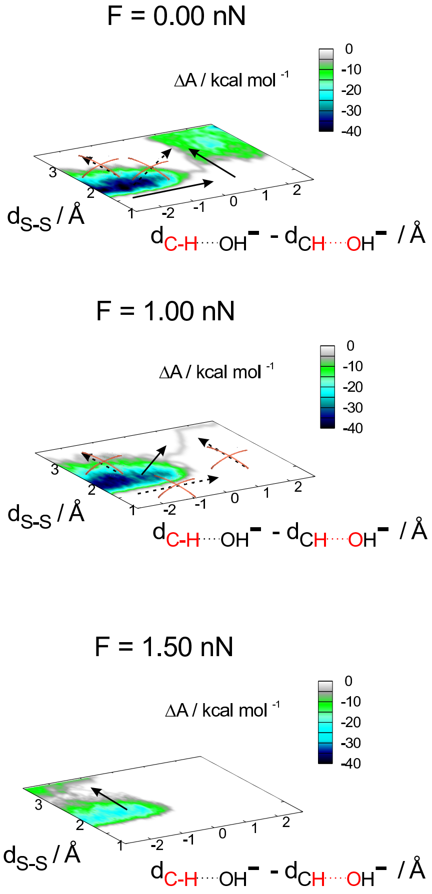

FIG. 4: **Change of the α-elimination reaction mechanism with applied force.** Force–transformed free energy surfaces for the attack of the OH^- anion to one of the α-hydrogen atoms in the absence of force, at 1.0 nN and at 1.5 nN external force at 300 K in aqueous solution. Black solid arrows highlight schematically the energetically preferred minimum free energy pathways according to the topology of the underlying free energy landscapes that depends on the magnitude of the constant external force, whereas dashed arrows and red crosses correspond to the disfavored mechanisms. Although the process is an elimination in the thermal limit ($F = 0$ nN) and at low forces, straightforward S–S bond rupture sets in upon reaching sufficiently large forces, $F > 1.5$ nN. In between, at a force of 1.0 nN, the synchronous single step elimination is observed.

and moderate–force regime akin to purely thermal activation.

Upon reaching forces exceeding about 1.5 nN, however, the gap between the activation free energies of the C–S bond rupture process and the S_N2 chemical reaction starts to be vanishingly small such that, at ~ 2 nN, the two reaction scenarios directly compete. Our simulations thus uncover that the mechanochemical event probed by experiments in this force regime is governed by two competitive mechanisms: a bimolecular S_N2 reaction involving a sulfur atom and a straightforward unimolecular C–S bond scission process. The observation that only the kinetics of the former reaction depends on the concentration of the attacking nucleophile, which is OH^-(aq), suggests that a series of new force–clamp AFM experiments at forces around ~ 2 nN conducted as a function of pH could confirm our predictions. Indeed, a rate of disulfide cleavage independent of pH would provide solid evidence that the probed process is simple unimolecular bond breaking. Remarkably, at only slightly higher forces of ~ 2.5 nN, unimolecular C–S bond rupture itself degenerates into an essentially barrierless and thus spontaneous process.

In addition to the competition between the S_N2 reaction and the C–S bond rupture process, which is characterized by the coexistence of these two channels at the same force, our simulations disclose that the external mechanical force is able to transform concerted pathways into two-step mechanisms. Indeed, at forces around 2.25 nN, the mechanism based on a S_N2 attack of OH^- at a sulfur atom transmutes into a direct S–S cleavage, followed by a decoupled OH^- addition to the generated cation, which is a barrierless process and it thus does not play any important role. In the metadynamics simulations carried out at and above the critical force of 2.25 nN, the reaction pathway associated with the bimolecular concerted S_N2 mechanism was never observed even if the simulation setup was flexible enough to enable that pathways (see subsection V.G of the Supporting Information). This strongly suggests that the transition state of the "S_N2 at S" pathway no longer exists above the critical force, which means that this very channel ceases to exist above this force. This gives rise to an intriguing topological scenario: below the critical force, both the "S_N2 at S" and the pure S–S bond breaking mechanisms exist as independent reaction channels. In contrast, at the critical force, the S_N2 pathway collapses into the S–S bond breaking pathway, being the latter type of pathway the only one that continues to exist for forces higher than the critical force. Hence, only one component of the reaction coordinate of the S_N2 mechanism (the component associated with S–S bond cleavage) survives beyond the critical force. It can thus be stated that the mechanical stress brings about a confluence of the "S_N2 at S" and S–S bond breaking pathways. The free energy landscapes of Figure 3 provide strong evidence that the external force is able to induce yet another confluence of mechanisms, namely the confluence of the "S_N2 at C" and C–S bond breaking pathways at around 1.25 nN. The fact that the activation free energy at zero force of the "S_N2 at C" channel lies quite close in energy to that of the preferred "S_N2 at S" pathway suggest that properly designed disulfide derivatives might enable new AFM experiments aimed at probing the latter confluence. Likewise, other disulfide molecules might also allow to probe the unique force–dependence of the activation free energy of the α–elimination mechanism in new AFM experiments.

Overall, an astonishingly rich reactivity scenario characterized by both confluence and competition of mechanisms is disclosed in the force window at roughly 1.5 ± 0.5 nN, which not only is at the heart of the force range that is realized in many state-of-the-art laboratory experiments in the realm of chemistry and biochemistry, but is also highly relevant for polymer–based materials whose mechanical properties under large stress depend on the mechanochemistry of their di- or polysulfide crosslinkers.

Thus, processes that are very unfavorable at certain forces outperform others beyond critical forces before these become superseded themselves. Ultimately, brute-force bond rupture processes seem to take over at about 2 to 2.5 nN in view of an increasingly favorable coupling of the mechanical coordinate to the reaction coordinate. It can be conjectured that all this is not the exception, but the rule for mechanically activated chemical reactions which underly sonochemistry and polymer mechanochemistry. In particular, these findings should be a warning to simplified interpretations of experimental data – even if presumably supported by standard quantum chemical calculations!

Computational methods

All isotensional AIMD simulations have been carried out using the Car–Parrinello propagation scheme based on density functional theory, pseudopotentials and plane waves as implemented in the `CPMD` program package.[39] The system contained one diethyl disulfide, one OH^- and 70 water molecules to properly solvate the reactants at 300 K subject to periodic boundary conditions. Metadynamics and thermodynamic integration have been used to sample free energies at constant external forces. See Supporting Information for more details (including additional analyses and validation of the electronic structure method) and references.

Acknowledgements

We are grateful to Deutsche Forschungsgemeinschaft (Reinhart Koselleck Grant "Understanding Mechanochemistry" (MA 1547/9) and Cluster of Excellence "RESOLV" (EXC 1069)), Alexander von Humboldt Stiftung (Humboldt Fellowships to J.R.A), Spanish Government (Ramón y Cajal Fellowship to J.R.A.), National Science Center Poland under Grant No. 2014/13/B/ST4/05009 and Ministry of Science and Higher Education Poland under Grant No. 627/STYP/9/2014 (Fellowships to P.D) for partial financial support. The authors gratefully acknowledge the Gauss Centre for Supercomputing (GCS) for providing computing time for a GCS Large Scale Project on JUQUEEN at Jülich Supercomputing Centre (JSC) as well as additional computational support by BOVILAB@RUB, HPC–RESOLV, Rechnerverbund–NRW, Wroclaw Supercomputer Center (WCSS), Galera–ACTION Cluster, and Academic Computer Center in Gdańsk (CI TASK).

Author contributions

P.D, J.R.-A. and D.M. conceived and designed the research; P.D performed the calculations; P.D, J.R.-A., P.A., M.K. and

D.M. analyzed the data; P.D., J.R.-A. and D.M. co-wrote the paper.

---

[*] Electronic address: `przemyslaw.dopieralski@theochem.rub.de`

[†] Electronic address: `jribasjr@yahoo.es`

[1] Beyer, M. K. & Clausen-Schaumann, H. Mechanochemistry: the mechanical activation of covalent bonds. *Chem. Rev.* **105**, 2921–2948 (2005).

[2] Caruso, M. M. *et al.* Mechanically–induced chemical changes in polymeric materials. *Chem. Rev.* **109**, 5755–5798 (2009).

[3] Black, A. L., Lenhardt, J. M. & Craig, S. L. From molecular mechanochemistry to stress–responsive materials. *J. Mater. Chem.* **21**, 1655–1663 (2011).

[4] Huang, Z. & Boulatov, R. Chemomechanics: chemical kinetics for multiscale phenomena. *Chem. Soc. Rev.* **40**, 2359–2384 (2011).

[5] Ribas-Arino, J. & Marx, D. Covalent mechanochemistry: theoretical concepts and computational tools with applications to molecular nanomechanics. *Chem. Rev.* **112**, 5412–5487 (2012).

[6] Wiita, A. P., Ainavarapu, S. R. K., Huang, H. H. & Fernandez, J. M. Force–dependent chemical kinetics of disulfide bond reduction observed with single–molecule techniques. *Proc. Natl. Acad. Sci. USA* **103**, 7222–7227 (2006).

[7] Wiita, A. P. *et al.* Probing the chemistry of thioredoxin catalysis with force. *Nature* **450**, 124–127 (2007).

[8] Ainavarapu, S. R. K., Wiita, A. P., Dougan, L., Uggerud, E. & Fernandez, J. M. Single–molecule force spectroscopy measurements of bond elongation during a bimolecular reaction. *J. Am. Chem. Soc.* **130**, 6479–6487 (2008).

[9] Liang, J. & Fernandez, J. M. Mechanochemistry: one bond at a time. *ACSNano* **3**, 1628–1645 (2009).

[10] Garcia-Manyes, S., Liang, J., Szoszkiewicz, R., Kuo, T. L. & Fernandez, J. M. Force–activated reactivity switch in a bimolecular chemical reaction. *Nat. Chem.* **1**, 236–242 (2009).

[11] Alegre-Cebollada, J., Kosuri, P., Rivas-Pardo, J. A. & Fernandez, J. M. Direct observation of disulfide isomerization in a single protein. *Nat. Chem.* **3**, 882–887 (2011).

[12] Garcia-Manyes, S., Kuo, T.-L. & Fernandez, J. M. Contrasting the individual reactive pathways in protein unfolding and disulfide bond reduction observed within a single protein. *J. Am. Chem. Soc.* **133**, 3104–3113 (2011).

[13] Liang, J. & Fernandez, J. M. Kinetic measurements on single–molecule disulfide bond cleavage. *J. Am. Chem. Soc.* **133**, 3528–3534 (2011).

[14] Popa, I., Kosuri, P., Alegre-Cebollada, J., Garcia-Manyes, S. & Fernandez, J. M. Force dependency of biochemical reactions measured by single-molecule force-clamp spectroscopy. *Nat. Protoc.* **8**, 1261–1276 (2013).

[15] Szoszkiewicz, R. Single-molecule studies of disulfide bond reduction pathways used by human thioredoxin. *Biophys. Chem.* **173–174**, 31–38 (2013).

[16] Kucharski, T. J. *et al.* Kinetics of thiol/disulfide exchange correlate weakly with the restoring force in the disulfide moiety. *Angew. Chem. Int. Ed.* **48**, 7040–7043 (2009).

[17] Tian, Y., Kucharski, T. J., Yang, Q. Z. & Boulatov, R. Model studies of force-dependent kinetics of multi-barrier reactions. *Nat. Commun.* **4:2538**, doi:10.1038/ncomms3538 (2013).

[18] Hofbauer, F. & Frank, I. Disulfide bond cleavage: a redox reaction without electron transfer. *Chem. Eur. J.* **16**, 5097–5101 (2010).

[19] Li, W. & Gräter, F. Atomistic evidence of how force dynamically regulates thiol/disulfide exchange. *J. Am. Chem. Soc.* **132**, 16790–16795 (2010).

[20] Iozzi, M. F., Helgaker, T. & Uggerud, E. Influence of external force on properties and reactivity of disulfide bonds. *J. Phys. Chem. A* **115**, 2308–2315 (2011).

[21] Baldus, I. B. & Gräter, F. Mechanical force can fine-tune redox potentials of disulfide bonds. *Biophys. J.* **102**, 622–629 (2012).

[22] Keten, S., Chou, C.-C., van Duin, A. C. & Buehler, M. J. Tunable nanomechanics of protein disulfide bonds in redox microenvironments. *J. Mech. Behav. Biomed. Mater.* **5**, 32 – 40 (2012).

[23] Hofbauer, F. & Frank, I. CPMD simulation of a bimolecular chemical reaction: nucleophilic attack of a disulfide bond under mechanical stress. *Chem. Eur. J.* **18**, 16332–16338 (2012).

[24] Dopieralski, P. *et al.* The Janus-faced role of external forces in mechanochemical disulfide bond cleavage. *Nat. Chem.* **5**, 685–691 (2013).

[25] Anjukandi, P., Dopieralski, P., Ribas-Arino, J. & Marx, D. The effect of tensile stress on the conformational free energy landscape of disulfide bonds. *PLOS ONE* **9**, e108812–1–7 (2014).

[26] Zhou, B., Baldus, I. B., Li, W., Edwards, S. A. & Gräter, F. Identification of allosteric disulfides from prestress analysis. *Biophys. J.* **107**, 672–681 (2014).

[27] Wouters, M. A., Fan, S. W. & Haworth, N. L. Disulfides as redox switches: from molecular mechanisms to functional significance. *Antioxidants & Redox Signaling* **12**, 53–91 (2010).

[28] Matthias, L. J. *et al.* Disulfide exchange in domain 2 of CD4 is required for entry of HIV–I. *Nat. Immunol.* **3**, 727–732 (2002).

[29] Hogg, P. J. Disulfide bonds as switches for protein function. *Trends in Biochemical Sciences* **28**, 210–214 (2003).

[30] Ahamed, J. *et al.* Disulfide isomerization switches tissue factor from coagulation to cell signaling. *Proc. Natl. Acad. Sci. USA* **103**, 13932–13937 (2006).

[31] Schmidt, B., Ho, L. & Hogg, P. J. Allosteric disulfide bonds. *Biochemistry* **45**, 7429–7433 (2006).

[32] Guo, X., Xiang, D., Duan, G. & Mou, P. A review of mechanochemistry applications in waste management. *Waste Management* **30**, 4–10 (2010).

[33] Zhang, X., Lu, Z., Tian, D., Li, H. & Lu, C. Mechanochemical devulcanization of ground tire rubber and its application in acoustic absorbent polyurethane foamed composites. *J. Appl. Polym. Sci.* **30**, 4006–4014 (2013).

[34] Rust, H. Non-chemical, mechanical procedure for the devulcanization of scrap rubber and/or elastomers and apparatus therefor (2015). URL `http://www.google.com/patents/US8957119`. US Patent 8,957,119.

[35] Mars, W. V. & Fatemi, A. Factors that affect the fatigue life of rubber: A literature survey. *Rubber Chem. Technol.* **77**, 391–412 (2004).

[36] Persson, B. N. J., Albohr, O., Heinrich, G. & Ueba, H. Crack propagation in rubber-like materials. *J. Phys.: Condens. Matter* **17**, R1071–R1142 (2005).

[37] Barcan, G. A., Zhang, X. & Waymouth, R. Structurally dynamic hydrogels derived from 1,2–dithiolanes. *J. Am. Chem. Soc.* **137**, 5650–5653 (2015).

[38] An, S. Y., Arunbabu, D., Noh, S. M., Song, Y. K. & Oh, J. K. Recent strategies to develop self–healable crosslinked polymeric networks. *Chem. Commun.* **51**, 13058–13070 (2015).

[39] Marx, D. & Hutter, J. *Ab Initio Molecular Dynamics: Basic Theory and Advanced Methods* (Cambridge University Press, Cambridge, 2009).

[40] Krupicka, M. & Marx, D. Disfavoring mechanochemical reactions by stress–induced steric hindrance. *J. Chem. Theory and Comput.* **xx**, xx (in review).

[41] Parker, A. J. & Kharasch, N. The scission of the sulfur-sulfur bond. *Chem. Rev.* **59**, 583–628 (1959).

[42] Singh, R. & Whitesides, G. M. Thiol–disulfide interchange. In Patai, S. & Rappoport, Z. (eds.) *Supplement S: the chemistry of sulphur–containing functional groups*, 633–658 (John Wiley & Sons Ltd., 1993).

[43] Hayes, J. M. & Bachrach, S. M. Effect of micro and bulk solvation on the mechanism of nucleophilic substitution at sulfur in disulfides. *J. Phys. Chem. A* **107**, 7952–7961 (2003).

[44] Fernandes, P. A. & Ramos, M. J. Theoretical insights into the mechanism for thiol/disulfide exchange. *Chem. Eur. J.* **10**, 257–266 (2004).

[45] Bach, R. D., Dmitrenko, O. & Thorpe, C. Mechanism of thiolate-disulfide interchange reactions in biochemistry. *J. Org. Chem.* **73**, 12–21 (2008).

[46] Swan, J. M. Mechanism of alkaline degradation of cystine residues in protein. *Nature* **179**, 965 (1957).

[47] Cecil, R. & McPhee, J. R. The sulfur chemistry of proteins. *Adv. Protein Chem.* **14**, 255–389 (1959).

[48] Florence, T. M. Degradation of protein disulphide bonds in dilute alkali. *Biochem. J.* **189**, 507–520 (1980).

[49] Grabowski, J. J. & Zhang, L. Dimethyl disulfide: Anion-molecule reactions in the gas phase at 300 K. *J. Am. Chem. Soc.* **111**, 1193–1203 (1989).

[50] Bachrach, S. M. & Pereverzev, A. Competing elimination and substitution reactions of simple acyclic disulfides. *Org. Biomol. Chem.* **3**, 2095–2101 (2005).

[51] Tarbell, D. & Harnish, D. Cleavage of the carbon–sulfur bond in divalent sulfur compounds. *Chem. Rev.* **49**, 1–90 (1951).

[52] Paranjothy, M., Siebert, M. R., Hase, W. L. & Bachrach, S. M. Mechanism of thiolate-disulfide exchange: Additionelimination or effectively S$_N$2? Effect of a shallow intermediate in gas-phase direct dynamics simulations. *J. Phys. Chem. A* **116**, 11492–11499 (2012).

[53] Heverly-Coulson, G. S., Boyd, R. J., Mó, O. & Yáñez, M. Revealing unexpected mechanisms for nucleophilic attack on S–S and Se–Se bridges. *Chem. Eur. J.* **19**, 3629–3638 (2013).

[54] Ribas-Arino, J., Shiga, M. & Marx, D. Understanding covalent mechanochemistry. *Angew. Chem. Int. Ed.* **48**, 4190–4193 (2009).

[55] Dopieralski, P., Ribas-Arino, J. & Marx, D. Force–transformed free energy surfaces and trajectory shooting simulations reveal the mechano–stereochemistry of cyclopropane ring–opening reactions. *Angew. Chem. Int. Ed.* **50**, 7105–7108 (2011).

[56] Marx, D., Chandra, A. & Tuckerman, M. E. Aqueous basic solutions: hydroxide solvation, structural diffusion, and comparison to the hydrated proton. *Chem. Rev.* **110**, 2174–2216 (2010).

[57] Bachrach, S. M. *Computational organic chemistry* (John Willey & Sons, New Jersey, 2007).

[58] Mohamed, A. A. & Jensen, F. Steric effects in S$_N$2 reactions. The influence of microsolvation. *J. Phys. Chem. A* **105**, 3259–3268 (2001).

[59] Dopieralski, P., Ribas-Arino, J., Anjukandi, P., Krupicka, M. & Marx, D. Force–induced reversal of β–eliminations: stressed disulfide bonds in alkaline solution. *Angew. Chem. Int. Ed.* **54**, 10.1002/anie.201508005 (2015).